

Ferroelastic Phase Transition of $\text{Cs}_3\text{H}(\text{SeO}_4)_2$

Eisuke Magome and Masaru Komukae

Department of Applied Physics, Tokyo University of Science, Kagurazaka, Shinjuku, Tokyo 162-8601, Japan

Fax: 81-3-3260-4772, e-mail: magome@rs.kagu.tus.ac.jp

Optical observation of twin structures and X-ray examinations of $\text{Cs}_3\text{H}(\text{SeO}_4)_2$ were carried above room temperature. Possible motional states of SeO_4^{2-} tetrahedra and hydrogen bonds above the ferroelastic phase transition point were studied by taking account of the results deduced for rearrangements of SeO_4^{2-} tetrahedra and hydrogen bonds accompanied by the movements of all ferroelastic domain boundaries. It was deduced that the dynamic orientational disordering of the SeO_4^{2-} tetrahedra give rise to both the perpetual breaking of hydrogen bond and the proton hopping motion among the 3-fold equivalent positions. Key words: domain, ferroelastic, $\text{Cs}_3\text{H}(\text{SeO}_4)_2$, proton, crystal structure

1. INTRODUCTION

Since the discovery of ferroelectric activity of triammonium hydrogen disulphate $(\text{NH}_4)_3\text{H}(\text{SO}_4)_2$ below room temperature [1], the crystals with alkali metal which belong to members of the family of hydrogen bonds compounds with the general formula $\text{M}_3\text{H}(\text{XO}_4)_2$ ($\text{M} = \text{K}, \text{NH}_4, \text{Cs}$ and $\text{X} = \text{S}, \text{Se}$) have been investigated with much interest [2-10]. The both crystals of $\text{K}_3\text{H}(\text{SeO}_4)_2$ and $\text{Cs}_3\text{H}(\text{SeO}_4)_2$ become antiferroelectric below 21 K and 51 K, respectively, and $(\text{NH}_4)_3\text{H}(\text{SeO}_4)_2$ ferroelectric below 181 K [11-13]. These phase transition points are increased by deuteration, showing a large isotope effect, while $\text{Rb}_3\text{H}(\text{SeO}_4)_2$ does not exhibit any phase transition down to 4.2 K, but phase transition is induced by deuteration [14]. It is, therefore, suggested that the proton motion between two sites within hydrogen bond connecting to oxygen atoms plays an important role in ferroelectric or antiferroelectric phase transition in $\text{M}_3\text{H}(\text{XO}_4)_2$ type crystals. It is well known that the crystals of $\text{M}_3\text{H}(\text{XO}_4)_2$ type undergo a ferroelastic phase transition above room temperature [15-17] and exhibit a high value in electric conductivity [18-20] as well as in the cases of CsHSO_4 [21,22] and CsHSeO_4 [22].

All ferroelastic phase transitions of $\text{M}_3\text{H}(\text{XO}_4)_2$ type crystals are characterized by symmetry change from trigonal with the space group $\text{R}\bar{3}\text{m}$ to monoclinic with A2/a [15,16].

It was found by the dielectric measurement that $\text{Cs}_3\text{H}(\text{SeO}_4)_2$ undergoes successive phase transitions at 451 K (T_1), 364 K (T_2) and 50 K (T_N), and phases are denoted as I, II, III and IV in order of descending temperature [12]. $\text{Cs}_3\text{H}(\text{SeO}_4)_2$ also undergoes a ferroelastic phase transition at 451 K caused by symmetry change from $\text{R}\bar{3}\text{m}$ to A2/a , the space group in the phase III is C2/m which differs from the space group [15,16] at room temperature of all other members.

It was reported by Komukae *et al.* that the hydrogen bonds of CsHSeO_4 are instantaneously broken and the protons are hopping among only the 16-fold equivalent positions above ferroelastic phase transition point. In dealing with motions of SeO_4^{2-} tetrahedra, it is often preferable to investigate the crystals of $\text{M}_3\text{H}(\text{XO}_4)_2$ type

instead of the crystals of MHXO_4 type, because CsHSeO_4 [24] and CsHSO_4 [25] have large spontaneous strains associated with its ferroelastic phase transition.

In order to make clear the mechanism of the ferroelastic phase transition in $\text{Cs}_3\text{H}(\text{SeO}_4)_2$, optical observation of twin structure, X-ray examinations were carried out above room temperature.

The present paper reports the possible motional states of SeO_4^{2-} tetrahedra and hydrogen above the ferroelastic phase transition point on the basis of both the crystal structure and the domain structure of $\text{Cs}_3\text{H}(\text{SeO}_4)_2$ observed at room temperature.

2. EXPERIMENTAL

The single crystals of $\text{Cs}_3\text{H}(\text{SeO}_4)_2$ were grown by evaporation method from aqueous solution of Cs_2SeO_4 and H_2SeO_4 in the molar ratio of 3:1. The crystals were recrystallized for purification. As-grown crystals of $\text{Cs}_3\text{H}(\text{SeO}_4)_2$ are of pseudo-hexagonal plate with the predominant faces of (001) and are transparent. Optical observations under a polarizing microscope showed that the crystals thus grown are optically biaxial, and frequently have domain structures at room temperature. The Weissenberg photographs were taken around the crystallographic a , b and c axes. The X-ray measurements were carried out by using the single crystals. Intensity data for the determination of the crystal structure were collected on Rigaku AFC-5 automatic four-circle diffractometer with graphite-monochromator using $\text{MoK}\alpha$ ($\lambda = 0.7107 \text{ \AA}$). A nearly spherical single crystal with a diameter $2r = 0.4 \text{ mm}$ was used as a specimen. The scanning speed was 4 deg/min. As a check on the stability of the crystal and the instruments, three standard reflections, $71\bar{4}$, $62\bar{2}$ and 530 were monitored every 100 reflections and no significant variation was noticed in their intensities. The intensity data were collected for $4^\circ < 2\theta < 65^\circ$ by the ω - 2θ scanning technique.

Corrections were made for Lorentz and polarization factors. Correction was also made for the linear absorption ($\mu_r = 3.5$ for $\text{MoK}\alpha$). 1837 independent reflections were measured, of those, 42 were omitted by the extinction effect. Finally 777 reflections with

values of $|F_o|$ greater than $3\sigma(|F_o|)$ were used for least-square calculations. In the final stage of refinement, the following weighting scheme was adopted: $w = (48.0/|F_o|)^2$ for $|F_o| \geq 48.0$, $w = 1$ for $|F_o| < 48.0$.

3. EXPERIMENTAL RESULTS

3.1 Observation of domain structures

It was found by optical observations of $Cs_3H(SeO_4)_2$ under a polarizing microscope that the crystal at room temperature shows twin structures composed of three kinds of crystallographic orientations named as domain D_1 , D_2 and D_3 , with two types of domain boundaries. One type of domain boundaries was found to be classified as a reflection twin plane parallel to $(31\bar{1})$ or $(\bar{3}11)$ plane which is almost perpendicular to the (001) plane. The other type was found to belong to a crystallographically non-prominent plane with $[110]$ or $[\bar{1}\bar{1}0]$ rotation axis, and tilted considerably from the normal to the (001) plane. The former and the latter are denoted as W- and W'-boundaries, respectively, according to Sapriel [32].

The ferroelastic domain structure at room temperature shown in Fig. 1 is interpreted on the basis of the mechanical twinning theory by taking account of the symmetry change from $\bar{3}/m$ to $2/m$ [31,32].

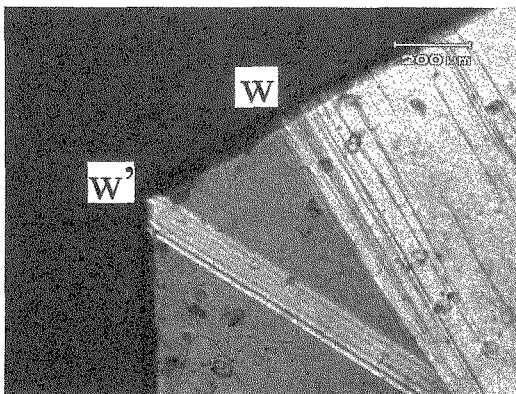


Fig. 1 Domain structure with three kinds of domains and two types of domain boundaries (W and W') viewed along the direction perpendicular to the (001) plane.

It was also found by optical observations that the domain structure in the phase II is composed of the same three kinds of orientation with two types of domain boundaries, as in the case of the phase III. The results in optical observations of domain structure point out that the point group of both the phases III and II are identical. The extinction position viewed only along the b_{mc} axis changes rapidly at the II-III phase transition point when the crystal is warmed up through the II-III phase transition point. The results obtained from optical observations are compatible with the relation of the unit cell parameters between the phases II and III. W'-boundary plane can not be simply indexed by a crystallographical prominent plane.

The components of the strain tensor a_s and c_s can be related to the lattice constants by

$$a_s = \frac{e_{22} - e_{11}}{2} = \frac{1}{2} - \frac{a_{mc}}{2\sqrt{3}b_{mc}}$$

$$c_s = e_{13} = \frac{a_{mc} + 3c_{mc} \cos \beta}{6c_{mc} \sin \beta}$$

The components of the strain tensor for $Cs_3H(SeO_4)_2$ are listed in table I, where those reported for other $M_3H(XO_4)_2$ type crystals [15,16] and other related materials [24,33] are shown for comparison. The comparisons of the strain tensor in the cases of $M_3H(XO_4)_2$ type crystals have a magnitude of order of 10^{-3} .

Table I. Components of spontaneous tensor in $M_3H(SeO_4)_2$ and other related material.

Crystal	$a_s = (e_{22} - e_{11})/2$	$c_s = e_{13}$
$Cs_3H(SeO_4)_2$	2.3×10^{-3}	7.1×10^{-3} (400 K)
	7.9×10^{-3}	-2.6×10^{-2} (300 K)
$(NH_4)_3H(SeO_4)_2$	-3.0×10^{-3}	3.3×10^{-3}
$K_3H(SeO_4)_2$	4.8×10^{-3}	-5.1×10^{-3}
$Rb_3H(SeO_4)_2$	3.5×10^{-3}	1.6×10^{-3}
$Pb_3(PO_4)_2$	2.2×10^{-2}	6.6×10^{-3}
$CsHSrSeO_4$	7.6×10^{-2}	2.7×10^{-2}

The possible orientations of the domain boundaries can be derived according to Sapriel's method based on the requirement that the spontaneous strain tensor must be mutually compatible on the boundary between any two adjacent domains [31]. We get the set of orientations of domain boundaries

$$x_2 = 0 \quad \text{and} \quad x_3 = -\frac{a_s}{c_s}x_1 \quad \text{for } D_2 \text{ and } D_3$$

$$x_2 = \sqrt{3}x_1 \quad \text{and} \quad \sqrt{3}x_2 + x_1 = -\frac{2c_s}{a_s}x_3 \quad \text{for } D_3 \text{ and } D_1$$

$$x_2 = -\sqrt{3}x_1 \quad \text{and} \quad \sqrt{3}x_2 - x_1 = -\frac{2c_s}{a_s}x_3 \quad \text{for } D_1 \text{ and } D_2$$

These orientations correspond well to our results of optical observation.

3.2 Crystal structure at room temperature

We have examined the crystal structure of $Cs_3H(SeO_4)_2$ at room temperature in order to discuss rearrangements of constituent ions accompanied by the movement of domain boundaries in ferroelastic phase. The lattice parameters in the phase II and III are $a_{ma} = 11.04 \text{ \AA}$, $b_{ma} = 6.403 \text{ \AA}$, $c_{ma} = 16.011 \text{ \AA}$, $\beta_{ma} = 102.8^\circ$ and $Z = 4$, and $a_{mc} = 10.879 \text{ \AA}$, $b_{mc} = 6.382 \text{ \AA}$, $c_{mc} = 8.437 \text{ \AA}$, $\beta_{mc} = 112.4^\circ$ and $Z = 2$, respectively.

The crystal structure of $Cs_3H(SeO_4)_2$ at room temperature was determined on the basis of the space group $C2/m$. First, the positions of all atoms of $Cs_3H(SeO_4)_2$ except by the hydrogen atoms were determined by Fourier synthesis. The atomic coordinates and the individual isotopic temperature

factors were then refined by a block-diagonal least-square method. Refinements were constituted until all parameter shifts become less than three times of their standard deviations. The final discrepancy factor R was deduced to 0.061. The projections at room temperature along b_{mc} and c_{mc} axes are illustrated in Fig.2. Calculation of the O-O distances as hydrogen bond length revealed that only the bond length of $O(1)-O(1)^{\alpha}$ shown by chain lines has a reasonable value of 2.54(3) Å, while the other O-O distance are greater than 3 Å. It can therefore be confirmed that neighboring SeO_4^{2-} tetrahedra are linked together in pairs by a hydrogen bonds, and $Cs_3H(SeO_4)_2$ exhibits a character of arrangement of hydrogen bonds parallel to the (010) plane, as shown in Fig.2. It is also interesting to note that the SeO_4^{2-} tetrahedra in the phase III are tilted out of the (001) plane.

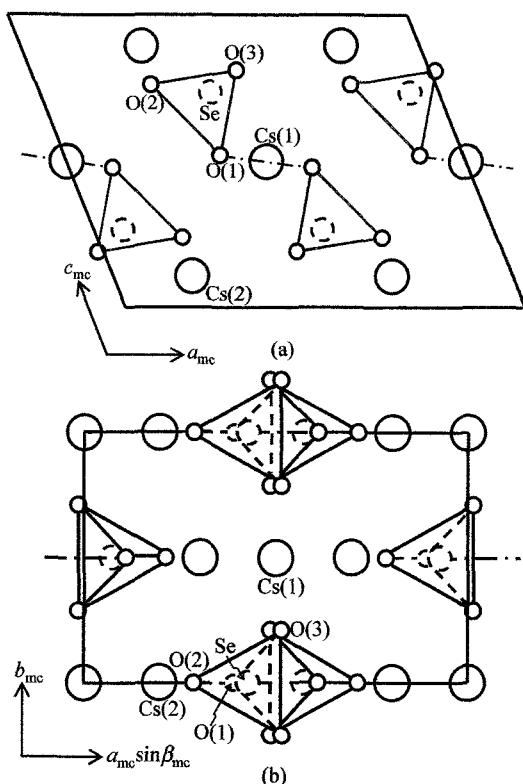


Fig.2 Crystal structure of $Cs_3H(SeO_4)_2$. (a) projection along the monoclinic b_{mc} axis. (b) projection along the monoclinic c_{mc} axis. The chain lines represent the hydrogen bonds.

3.3 Crystal Structure in Praelastic Phase

Because a domain boundary separating domains disappears when the crystal is warmed up through ferroelastic phase transitions point, SeO_4^{2-} tetrahedra and Cs ions an average structure of the praelastic phase should be expected to be located at least in the mean positions of the constituent ions of three kinds of crystallographic orientations. Although the ferroelastic phase transition occurs at T_1 , it is possible to estimate the crystal structure in the praelastic phase, on the basis of the crystal structure in the phase III

instead of the phase II. Because the space group $C2/m$ in the phase III is also a subgroup $R\bar{3}m$ in the phase I.

The arrangement of SeO_4^{2-} tetrahedra and Cs ions of the deduced crystal structure satisfies the symmetry of the space group $R\bar{3}m$ in the trigonal phase as shown in Fig.3. The crystal in the trigonal phase exhibits a character of 2-dimensional of hydrogen bonds, and the protons are continually hopping among the 3-fold equivalent positions accompanied by the breaking of hydrogen bond. The distance between the 3-fold equivalent positions shown by open circles was deduced to be 3.2 Å, which is considerably shorter than the layer distance 7.8 Å between hydrogen networks. Such a quasi two-dimensional network of hydrogen bonds in the trigonal phase was confirmed also in the cases of $K_3H(SeO_4)_2$ and $Rb_3H(SeO_4)_2$, by taking account of the crystal structure [34,35] with the space group $A2/a$ at room temperature.

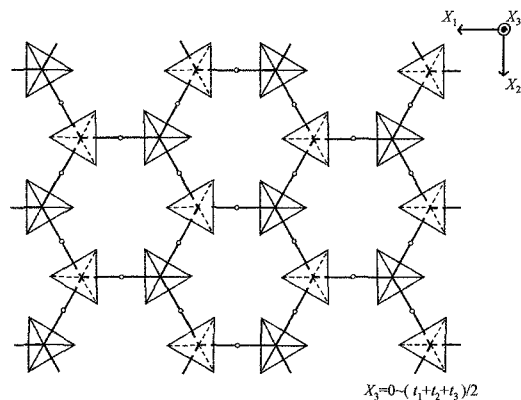


Fig.3 Average crystal structure in the Phase I deduced by taking account of the mean positions of the constitute ions of all domain.

The O-O distance of hydrogen bonds from the geometrical average structure in the trigonal phase turn out to be 3.8 Å, which is a reasonable value as hydrogen bond length compared with O-O distance 2.54 Å at room temperature and 2.65 Å in the $A2/a$ phase. There exists a large discrepancy between the O-O distance value of 3.8 Å estimated as a geometrical average structure and 2.71 Å reported by Merinov *et al.*²⁸⁾ Merinov *et al.* reported that the vertex oxygen of the SeO_4^{2-} tetrahedra is disordered with population coefficient of 1/3 over the three possible symmetry equivalent positions, while the oxygens of the base of the tetrahedra execute anharmonic thermal vibrations.²⁸⁾

It can be suggested from the magnitude of the O-O distance and the twinning conditions that SeO_4^{2-} tetrahedra in the praelastic phase have dynamically three kinds of structurally equivalent orientations, which are statically observed as ferroelastic domain structure as shown in Fig.4. It was therefore deduced that the dynamic

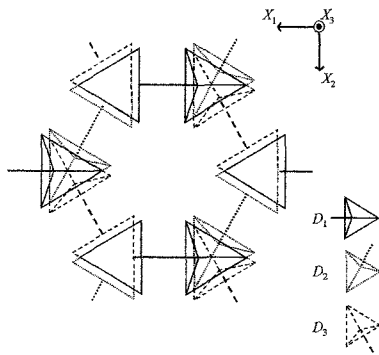


Fig.4 Crystal structure in the Phase I finally deduced. Three kinds of structurally equivalent orientation of the SeO_4^{2-} tetrahedra are shown.

orientational disordering of SeO_4^{2-} tetrahedra gives rise to both the perpetual breaking of hydrogen bonds and the proton hopping motion among only the 3-fold equivalent positions. It can be expected from the disordering of SeO_4^{2-} tetrahedra in three kinds of orientations above T_1 that the entropy change accompanied the ferroelastic phase transition in $M_3H(XO_4)_2$ type crystals is to be $R \ln 3$.

REFERENCES

- [1] K. Gesi, *Phys. Status Solidi*, (a)**33**, 479 (1976).
- [2] T. Osaka, Y. Makita and K. Gesi, *J. Phys. Soc. Jpn.*, **43**, 933 (1977).
- [3] K. Gesi, *J. Phys. Soc. Jpn.*, **43**, 1949 (1977).
- [4] S. Suzuki and Y. Makita, *Acta Crystallogr.*, **B34** 732 (1978).
- [5] T. Osaka, Y. Makita and K. Gesi, *J. Phys. Soc. Jpn.*, **46**, 577 (1979).
- [6] T. Osaka, Y. Oshino, K. Gesi and Y. Makita, *J. Phys. Soc. Jpn.*, **47**, 874 (1979).
- [7] K. Gesi, *J. Phys. Soc. Jpn.*, **48**, 886 (1979).
- [8] S. Suzuki, *J. Phys. Soc. Jpn.*, **47**, 1205 (1979).
- [9] T. Osaka, Y. Makita and K. Gesi, *J. Phys. Soc. Jpn.*, **49**, 593 (1980).
- [10] T. Osaka, T. Sato and Y. Makita, *Ferroelectrics*, **55**, 283 (1984).
- [11] M. Endo, T. Kaneko, T. Osaka and Y. Makita, *J. Phys. Soc. Jpn.*, **52**, 3829 (1983).
- [12] M. Komukae, T. Osaka, T. Kaneko and Y. Makita, *J. Phys. Soc. Jpn.*, **54**, 3401 (1985).
- [13] K. Gesi, *J. Phys. Soc. Jpn.*, **42**, 1785 (1977).
- [14] K. Gesi, *J. Phys. Soc. Jpn.*, **50**, 3185 (1981).
- [15] S. Yokota, Y. Makita and Y. Takagi, *J. Phys. Soc. Jpn.*, **51**, 1461 (1982).
- [16] T. Kishimoto, T. Osaka, M. Komukae and Y. Makita, *J. Phys. Soc. Jpn.*, **56**, 2070 (1987).
- [17] B. V. Merinov, A. I. Baranov, A. V. Tregubchenko and L. A. Shuvalov, *Dokl. Akad. Nauk SSSR*, **302**, 1376 (1988).
- [18] A. I. Baranov, I. P. Makarova, L. A. Muradyan, A. V. Tregubchenko, L. A. Shuvalov and V. I. Simonov, *Kristallografiya*, **32**, 682 (1987).
- [19] A. I. Baranov, A. V. Tregubchenko, L. A. Shuvalov and N. M. Shchagina, *Fiz. Tverd. Tela (Leningrad)*, **29**, 2513 (1987).
- [20] A. I. Baranov, B. M. Merinov, A. V. Tregubchenko, L. A. Shuvalov and N. M. Schgina, *Ferroelectrics*, **81**, 187 (1988).
- [21] M. Komukae, T. Osaka, Y. Makita, T. Ozaki, K. Itoh and E. Nakamura, *J. Phys. Soc. Jpn.*, **50**, 3187 (1981).
- [22] A. I. Baranov, L. A. Shuvalov and N. M. Shchagina, *Pis'ma Zh. Eksp. Teor. Fiz.*, **36**, 381 (1982).
- [23] M. Komukae, M. Tanaka, T. Osaka, Y. Makita, K. Kozawa and T. Uchida, *J. Phys. Soc. Jpn.*, **59**, 197 (1990).
- [24] S. Yokota, *J. Phys. Soc. Jpn.*, **51**, 1884 (1982).
- [25] T. Ozaki, K. Itoh and E. Nakamura, *J. Phys. Soc. Jpn.*, **51**, 213 (1982).
- [26] T. Sakurai, K. Kobayashi, *Rep. Inst. Phys. & Chem. Res.*, **55**, 69 (1979).
- [27] B. V. Merinov, N. B. Bolotina, A. I. Baranov and L. A. Shuvalov, *Kristallografiya*, **33**, 1387 (1988).
- [28] B. V. Merinov, A. I. Baranov, and L. A. Shuvalov, *Kristallografiya*, **35**, 355 (1990).
- [29] B. V. Merinov, N. B. Bolotina, A. I. Baranov and L. A. Shuvalov, *Kristallografiya*, **36**, 1131 (1991).
- [30] M. Ichikawa, T. Gustafsson and I. Olovsson, *Acta Crystallogr.*, **B48**, 633 (1992).
- [31] J. Sapriel, *Phys. Rev.*, **B12**, 5128 (1975).
- [32] K. Aizu, *J. Phys. Soc. Jpn.*, **28**, 706 (1970).
- [33] E. F. Dudnik, S. A. Sushko, G. A. Kiosse and T. I. Malinovskiy, *Ferroelectrics*, **48**, 149 (1983).
- [34] M. Ichikawa, S. Sato, M. Komukae and T. Osaka, *Acta Crystallogr.*, **C48**, 1569 (1992).
- [35] I. P. Makarova, I. A. Verin and N. M. Shchagina, *Kristallografiya*, **31**, 178 (1986).

(Received December 10, 2005; Accepted January 31, 2006)